Binding of Protein Phosphatase 2A to the L-Type Calcium Channel $Ca_v1.2$ next to Ser1928, Its Main PKA Site, Is Critical for Ser1928 Dephosphorylation†

Duane D. Hall,‡ Joel A. Feekes,‡ Aruni S. Arachchige Don,‡ Mei Shi,‡ Jawed Hamid,§ Lina Chen,§ Stefan Strack,‡ Gerald W. Zamponi,§ Mary C. Horne,‡ and Johannes W. Hell*,‡

Department of Pharmacology, Roy J. and Lucille A. Carver College of Medicine, University of Iowa, Iowa City, Iowa 52242-1109, and Department of Physiology and Biophysics and Hotchkiss Brain Institute, University of Calgary, Calgary T2N 4N1, Canada

Received August 10, 2005; Revised Manuscript Received January 7, 2006

ABSTRACT: The cAMP-dependent protein kinase (PKA) controls a large number of cellular functions. One critical PKA substrate in the brain and heart is the L-type Ca^{2+} channel $Ca_v1.2$, the activity of which is upregulated by PKA. The main PKA phosphorylation site is serine 1928 in the central pore forming $\alpha_1$1.2 subunit of $Ca_v1.2$. PKA is bound to $Ca_v1.2$ within a macromolecular signaling complex consisting of the β_2 adrenergic receptor, trimeric G_s protein, and adenylyl cyclase for fast, localized, and hence specific signaling [Davare, M. A., Avdonin, V., Hall, D. D., Peden, E. M., Buret, A., Weinberg, R. J., Horne, M. C., Hoshi, T., and Hell, J. W. (2001) *Science* 293, 98−101]. Protein phosphatase 2A (PP2A) serves to effectively balance serine 1928 phosphorylation by PKA through its association with the $Ca_v1.2$ complex [Davare, M. A., Horne, M. C., and Hell, J. W. (2000) *J. Biol. Chem.* 275, 39710−39717]. We now show that native PP2A holoenzymes, as well as the catalytic subunit itself, bind to $\alpha_1$1.2 immediately downstream of serine 1928. Of those holoenzymes, only heterotrimeric PP2A containing B′ and B″ subunits copurify with $\alpha_1$1.2. Preventing the binding of PP2A by truncating $\alpha_1$1.2 28 residues downstream of serine 1928 hampers its dephosphorylation in intact cells. Our results demonstrate for the first time that a stable interaction of PP2A with $Ca_v1.2$ is required for effective reversal of PKA-mediated channel phosphorylation. Accordingly, PKA as well as PP2A are constitutively associated with $Ca_v1.2$ for its proper regulation by phosphorylation and dephosphorylation of serine 1928.

Voltage-gated Ca^{2+} channels are formed by a central α_1 subunit, which constitutes the ion-conducting pore, in association with auxiliary α_2-δ, and β subunits (*1*). L-type channels are high threshold voltage-gated Ca^{2+} channels that are pharmacologically defined by their sensitivity to so-called organic calcium channel blockers such as nifedipine and exhibit relatively long-lasting openings. $Ca_v1.2$ and $Ca_v1.3$, formerly known as class C and D Ca^{2+} channels, contain $\alpha_1$1.2 and $\alpha_1$1.3 as central subunits, respectively. $Ca_v1.2$ is the prevailing L-type channel not only in the cardiovascular system and the heart but also in the brain (*2*, *3*). Ca^{2+} influx through L-type channels is involved in the regulation of a variety of functions including membrane excitability (*4*), synaptic plasticity (*5*−*8*), and gene expression (*9*, *10*). In the heart, Ca^{2+} influx through $Ca_v1.2$ is the critical first step that triggers myocardial contraction.

The β-adrenergic signaling pathway increases the heart rate in part by cAMP-dependent protein kinase (PKA)[1]-mediated phosphorylation of $Ca_v1.2$ (*11*), which enhances the activity of the channel (*12*, *13*). Phosphorylation of $\alpha_1$1.2 is sufficient for the upregulation of channel activity by PKA (*14*), although phosphorylation of a β subunit may also contribute (*15*). PKA phosphorylates $\alpha_1$1.2 at serine 1928 *in vitro* and *in vivo* (*11*, *16*−*20*). Gao et al. reported that mutation of serine 1928 to alanine inhibits PKA-mediated phosphorylation of $\alpha_1$1.2 and upregulation of $\alpha_1$1.2 channel activity (*21*). Serine 1928 is only present in the full-length 220 kDa form of $\alpha_1$1.2. In neurons, Ca^{2+} influx through NMDA-type glutamate receptors induces cleavage of full-length $\alpha_1$1.2 by the Ca^{2+}-activated protease calpain upstream of serine 1928, which creates the 180 kDa short form of $\alpha_1$1.2 (*22*, *23*). C-Terminal truncation in the region where calpain cleaves $\alpha_1$1.2 increases $Ca_v1.2$ activity about 4-fold (*24*). This modification is permanent in contrast to the phosphorylation by PKA, which is readily reversed by protein

† This work was supported by the National Institute of Health Research Grants R01-NS35563 (to J.W.H.), R01-GM56900 (to M.C.H.), R01-NS43254 (to S.S.), the American Heart Association Grant AHA0455653Z (to S.S.), an operating grant from the Canadian Institutes of Health Research (to G.W.Z.). G.W.Z. is a Canada Research Chair in Molecular Neurobiology and a Senior Scholar of the Alberta Heritage Foundation for Medical Research. D.D.H. and M.S. were supported by the NIH Training Grant T32 HL07121. D.D.H. was also supported by NIH Training Grants T32 DK07759 and T32 AG00213.

* To whom correspondence should be addressed: Department of Pharmacology, Roy J. and Lucille A. Carver College of Medicine, University of Iowa, 51 Newton Road, 2-512 BSB, Iowa City, IA 52242-1109. Telephone: (319) 384-4732. Fax: (319) 335-8930. E-mail: johannes-hell@uiowa.edu.

‡ University of Iowa.

§ University of Calgary.

[1] Abbreviations: PKA, cAMP-dependent protein kinase; AKAP, A-kinase anchor protein; DTT, dithiothreitol; MAP, microtubule-associated protein; SDS, sodium dodecyl sulphate; PAGE, polyacrylamide gel electrophoresis; GST, glutathione-*S* transferase; PCR, polymerase chain reaction; DMEM, Dulbecco's modified Eagle medium.

10.1021/bi051593z CCC: $33.50
Published on Web 02/15/2006

phosphatases. Okadaic acid inhibits the serine/threonine phosphatases, protein phosphatase 2A (PP2A) and, with a lower affinity, PP1. Its administration was found to upregulate the PKA-stimulated activity of $Ca_v1.2$, which had been ectopically expressed in Chinese hamster ovary (CHO) cells (*14*). Furthermore, an increase in phosphorylation of $\alpha_1 1.2$ ectopically expressed in HEK293 cells as published by Gao et al. was only detectable in the presence but not absence of phosphatase inhibitors upon increased cAMP production by forskolin-induced stimulation of adenylyl cyclase activity (*21*).

For fast and selective phosphorylation, PKA interacts with various substrates via a class of adaptor proteins called A-kinase anchor proteins (AKAPs) (*25*−*27*). Early functional studies indicated that disruption of the PKA−AKAP interaction inhibits the regulation of AMPA-type glutamate receptors (*28*) and skeletal muscle L-type channels ($Ca_v1.1$) (*29*) by PKA. PKA is constitutively associated with $Ca_v1.2$, which can bind three different AKAPs: AKAP15/18 (*30*), AKAP150 (Hall, D. D., Davare, M. A., Shi, M., and Hell, J. W., unpublished data) and its human homologue AKAP79 (*31*), and the otherwise microtubule-associated protein MAP2B (*18*), the first AKAP identified as such (*32*). PKA-mediated phosphorylation of $\alpha_1 1.2$ was observed when wild-type AKAP79 was coexpressed with $Ca_v1.2$ in HEK293 cells; this phosphorylation was not detectable when a mutant AKAP79 deficient for PKA binding was coexpressed (*21*). Accordingly, PKA anchoring at $\alpha_1 1.2$ is essential for its efficient phosphorylation and regulation. Previous studies indicated that phosphorylation and dephopshorylation of $\alpha_1 1.2$ is highly dynamic with phosphatases counteracting PKA very quickly (*14*, *33*). For example, okadaic acid substantially slowed the run-down of $Ca_v1.2$ activity that is typically observed in inside-out patches after excision from ventricular myocytes (*33*). These results suggest that a phosphatase was present in the patch.

We showed earlier that PP2A is constitutively bound to $Ca_v1.2$ and that channel-associated PP2A reverses phosphorylation of serine 1928 by PKA in immunoisolated $Ca_v1.2$ complexes (*19*). Now, we define the precise binding site for PP2A, which lies immediately downstream of serine 1928. Elimination of this site by truncating $\alpha_1 1.2$ 28 residues downstream of serine 1928 does not affect its phosphorylation by PKA but inhibits its dephosphorylation in intact cells. We conclude that a stable interaction of the PP2A holoenzyme with $Ca_v1.2$ is necessary for the phosphatase to effectively reverse serine 1928 phosphorylation by PKA.

EXPERIMENTAL PROCEDURES

Materials. Okadaic acid and a purified catalytic subunit of PKA were purchased from Sigma (St. Louis, MO); PP1 and PP2B were purchased from GloboZymes (Carlsbad, CA); microcystin-LR, fostriecin, cyclosporin A, protein phosphatase inhibitor-2, and cypermethrin were purchased from Calbiochem (San Diego, CA); and ECL and ECL-Plus detection kits, protein-G Sepharose, and glutathione Sepharose were purchased from Amersham Pharmacia Biotech (Piscataway, NJ). Protein-A Sepharose was obtained from Repligen (Waltham, MA). Other reagents were obtained from the usual commercial suppliers and were of standard biochemical quality.

Antibodies. The pan-specific antibody against the various PP2A B′ regulatory subunit isoforms was raised in rabbits by injecting an affinity-purified glutathione-*S* transferase (GST) fusion protein of residues 99−492 of B′δ [formerly called B′γ in rabbit (*34*); for the sequence, see GenBank accession number U38193]. This sequence is highly conserved between all known B′ regulatory subunit isoforms. Expression in *Escherichia coli* and purification on glutathione Sepharose was performed as described earlier (*35*). Immunization, serum collection and preparation, and affinity purification was analogous to those procedures detailed elsewhere (*2*, *36*, *37*). The following antibodies used in this study were previously described by us: the anti-$\alpha_1 1.2$ antibody was produced against a GST-fusion protein of the large cytosolic loop between domains II and III of $\alpha_1 1.2$ (*18*); the phosphospecific CH1923−1932P antibody (anti-$\alpha_1 1.2$-P) was raised against a peptide with the indicated residue sequence surrounding phosphorylated serine 1928 (*11*, *18*); and the anti-GST antibody was generously provided by Dr. J. W. Tracy (University of Wisconsin, Madison, WI) (*35*). The mouse monoclonal anti-PP2A/C antibody 1D6 (*38*) was purchased from Upstate Biotechnology (Lake Placid, NY); the polyclonal goat anti-PP2A/Aα antibody (*38*) was purchased from Santa Cruz Biotechnology (Santa Cruz, CA); and anti-PP1, a mouse monoclonal antibody (*39*), and anti-PP2B (*40*, *41*) antibodies were obtained from BD Transduction Laboratories. Specific antibodies against different PP2A B′ regulatory subunits (anti-B′α and anti-B′β) were a kind gift of Dr. D. M. Virshup (Huntsman Cancer Institute, University of Utah, Salt Lake City, UT). Specificity was confirmed in ectopic expression and RNAi experiments utilizing PC12 cells (*42*). The mouse polyclonal pan-B family antibody was raised against a GST-fusion protein containing the first 149 residues of the PP2A Bγ regulatory subunit. It recognizes an epitope common to the B family of the PP2A regulatory subunits (B$\alpha/\beta/\gamma/\delta$) but does not cross-react with B′ or B″ subunits (*43*). The rabbit polyclonal antipeptide antibody directed against B″β (PR59) was generously provided by Dr. E. Ogris (Vienna Biocenter, Vienna, Austria). Anti-PP5 was a gracious gift from Dr. S. Rossie (Purdue University, West Lafayette, IN) (*44*). Control purified rabbit IgG was purchased from Zymed Laboratories, Inc. (South San Francisco, CA), and control purified mouse IgG was purchased from Jackson ImmunoResearch Laboratories, Inc. (West Grove, PA).

Immunoprecipitation and Immunoblotting. All homogenization and immunoprecipitation procedures were performed at 4 °C. Rat forebrains (Harlan Sprague Dawley, 2−6 months old) were homogenized in 10 mL of ice-cold sucrose buffer (320 mM sucrose, 10 mM Tris-HCl at pH 7.4, plus protease inhibitors: 1 μg/mL pepstatin A, 10 μg/mL leupeptin, 20 μg/mL aprotinin, and 8 μg/mL each of calpain inhibitors I and II). The homogenate was spun for 2 min at 5000*g* in a Sorvall SS-34 rotor, and the supernatant was respun for 15 min at 250000*g* in a Beckman TLA-100.3 ultracentrifuge rotor. The supernatant from this spin contains cytosolic proteins and was used as a source of native phosphatases. The membrane pellet was resuspended in Triton X-100 solubilization buffer (10 mM Tris-HCl at pH 7.4, 150 mM NaCl, 1% Triton X-100, 10 mM EDTA, 5 mM EGTA, plus protease inhibitors), homogenized, and spun for 15 min at 250000*g* to obtain the detergent-soluble membrane fraction.

For HEK293 cells expressing ectopic HA-tagged B′ subunits, cells were lysed with RIPA buffer [10% glycerol, 1% NP-40, 150 mM NaCl, 50 mM Tris-HCl at pH 7.4, 5 mM EDTA, 5 mM EGTA, 0.4% deoxycholate, 0.05% sodium dodecyl sulphate (SDS), plus protease inhibitors] as described previously (*37*). For immunoprecipitation, 30 μL of prewashed protein-A or protein-G Sepharose slurry (50% resin and 50% liquid) and 5 μg of the indicated antibody per sample were incubated with homogenates for 3−6 h and washed 3 times with 0.1% Triton X-100 in TBS (10 mM Tris-HCl and 150 mM NaCl). Proteins were extracted in SDS sample buffer, ran on SDS−polyacrylamide gel electrophoresis (PAGE), transferred to PVDF membrane (0.2 μm, BioRad), and probed as previously described (*2*, *18*).

Construction of GST-Fusion Protein Vectors. Rat $\alpha_1$1.2 cDNA (*45*) was used as a template to construct five overlapping fragments of the $\alpha_1$1.2 C terminus as GST fusions. Oligonucleotides were designed with a *Bam*H I restriction site within the 5′ forward primer and an *Eco*R I restriction site followed by a V5 epitope tag within the 3′ reverse primer. All reverse primers began with the sequence 5′-GGC TGA ATT CCG TAG AAT CGA GAC CGA GGA GAC CGT TAG GGA TAG GCT TAC C-3′; the coding sequence for the V5 tag is underlined, and the reverse sequence annealing to $\alpha_1$1.2 follows the last nucleotide. For CT-A (residues 1584−1707), the forward primer was 5′-GCG AAT GGA TCC GTC GAC GAG CTG AGA GCC ATC ATC AAG-3′ and the rest of the reverse primer was 5′-GA CGT GGT TGC CAA ACA GGC CTC-3′; for CT-B (residues 1694−1817), the forward primer was 5′-CGG CAA GGA TCC GTC GAC GAC ATC TTC AGG AGG GCT GGA GG-3′ and the rest of the reverse primer was 5′-GT GGC ACC TCT TAG AGC TGA G-3′; for CT-C (residues 1804−1927), the forward primer was 5′-GCC GTC GGA TCC GTC GAC GTA CAG GAG GCA GCA TGG AAA CTC-3′ and the rest of the reverse primer was 5′-GT GAT GAA CCA GAT GCA AGG GC-3′; for CT-D (residues 1914−2037), the forward primer was 5′-CGC AGA GGA TCC GTC GAC ATC TCT CAG AAG ACA GCC TTG C-3′ and the rest of the reverse primer was 5′-CA GGC TGC TGG CGC TGC CG-3′; and for CT-E (residues 2024−2140), the forward primer was 5′-CCG AGA GGA TCC GTC GAC GGA GCT CCA GGC AGA CAG TTC C-3′ and the rest of the reverse primer was 5′-CA GGT TGC TGA CAT AGG ACC TGC-3′. Fragments were amplified using Clontech's HF-Advantage polymerase chain reaction (PCR) kit, purified with QIAGEN's QIAquick PCR purification kit, digested with *Bam*H I and *Eco*R I, and ligated into *Bam*H I/*Eco*R I digested pGEX4T1. Positive clones were verified via sequencing. The pTrc-HisA-PP2A/C 6×His-tagged fusion construct was described earlier by us (*19*). The GST-fusion constructs CT-1 (rabbit $\alpha_1$1.2 residues 1507−1733; for the sequence, see GenBank accession number CAA33546), CT-4 (1909−2171), CT-5 (1509−1622), CT-7 (2030−2171), CT-8 (1909−2029), CT-14 (1622−1733), and CT-23 (1622−1905) were generously provided by Dr. M. M. Hosey (Northwestern University, Chicago, IL) (*46*).

In Vitro Binding and Dephosphorylation Assays of GST-Fusion Proteins. The 6×His-PP2A/C construct (*37*) and $\alpha_1$1.2 GST-fusion proteins were expressed and purified from Nova Blue (Novagen, Madison, WI) and BL21 Star (Invitrogen, San Diego, CA) *E. coli* strains and used for *in vitro* interaction studies as described previously (*19*, *35*, *37*, *47*). Dephosphorylation assays were adapted from ref *19*, using brain cytosol as a source of native phosphatases. Immobilized GST-CT-4 fusion protein containing the serine 1928 PKA phosphorylation site residue was *in vitro* phosphorylated with PKA in phosphorylation buffer [50 mM HEPES−NaOH at pH 7.4, 10 mM $MgCl_2$, 0.1% Triton X-100, 1 mM EGTA, 400 μM dithiothreitol (DTT), 200 μM ATP, 1 μg/mL pepstatin A, 10 μg/mL leupeptin, 20 μg/mL aprotinin, and 1.5 μg/mL PKA] for 45 min at 32 °C with continuous agitation. Immobilized proteins were then washed 3 times in ice-cold kinase wash buffer (25 mM Tris-HCl at pH 7.4, 75 mM NaCl, 20 mM EDTA, and 0.1% Triton X-100). The cytosolic fraction from brain homogenate was obtained as above, except EDTA and EGTA was left out to not chelate Ca^{2+}. Cytosol was then diluted 15-fold in sucrose buffer and preincubated 30 min on ice with phosphatase inhibitors (50 mM NaF, 20 mM Na pyrophosphate, and 1 mM *p*-nitrophenyl phosphate), when used, before beginning the dephosphorylation reactions. Immobilized, phosphorylated fusion proteins were added to 500 μL of diluted cytosol at 37 °C for 45 min unless otherwise indicated. After 3 more washes with wash buffer, this time supplemented with phosphatase inhibitors, samples were analyzed by immunoblotting with antibodies against $\alpha_1$1.2-P, followed by reprobing with anti-GST. When phosphorylated fusion proteins were used in conjunction with immunoprecipitated or purified phosphatases (Figure 3), fusion proteins were first eluted from the resin and dialyzed. They were then *in vitro* phosphorylated as above in solution. PKA was inhibited by the addition of PKI (10 μM) before incubation with phosphatases. For dephosphorylation with purified phosphatases, 0.05 unit of PP1 or PP2B was added to 0.05 pmol of phosphorylated CT-4 in 50 mM Tris-HCl at pH 7.4 and 3 mM $MnCl_2$ per reaction; 1 mM $CaCl_2$ and 1 mM calmodulin was supplemented to the PP2B reactions.

For quantification, immunoblots were scanned using an Epson Perfection 4180 Photo flatbed scanner and phosphorylation levels were quantified via densitometry of the scanned immunosignals in Adobe Photoshop. We saw no difference in quantification when compared to densitometric analysis performed on a Kodak 440CF Image Station. The ratio of the anti-$\alpha_1$1.2-phosphosignal to the anti-GST signal of the GST-fusion proteins CT-4 was determined for each reaction. Ratios were normalized to the ratio of the pretreatment (no cytosol) sample within each experiment to provide a comparison between experiments. Means and errors (represented as SEMs) were calculated using one-way ANOVA with Prism 3.0 (GraphPad Software, Inc.). Values were deemed significant at $p < 0.05$ using the paired *t*-test method.

Expression of the Wild Type and C-Terminally Truncated $\alpha_1$1.2 Mutants in tsA-201 Cells. The wild-type rat $\alpha_1$1.2, rat β_{1b}, and rat α_2-δ_1 constructs were kindly donated by Dr. T. P. Snutch (University of British Columbia, Vancouver, Canada). The truncation mutants of the C-terminal region of $\alpha_1$1.2 stops 5−8 were generated by insertion of stop codons at positions immediately following residues 1889, 1956, 2026, and 2093 [rabbit $\alpha_1$1.2 sequence (*45*); see also Figure 1] using established mutagenesis procedures as will be described elsewhere (Gui, P., Wu, X, Ling, S., Stotz, S. C., Winkfein, R. J., Wilson, E., Davis, G. E., Braun, A. P.,

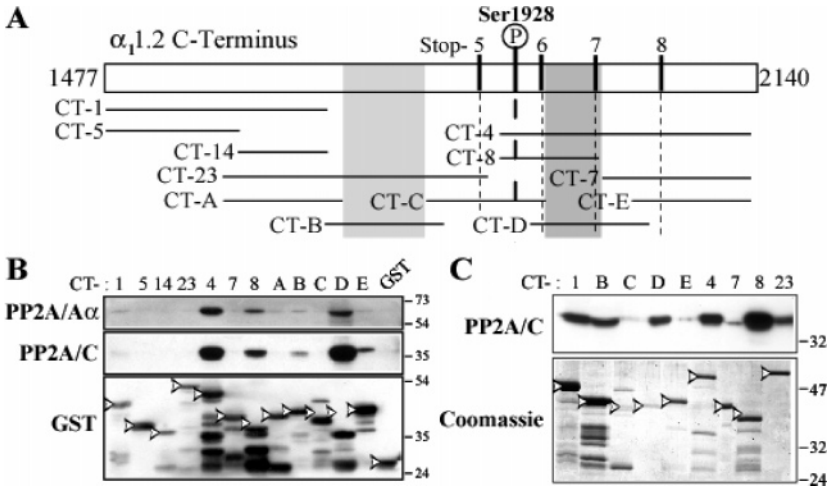

FIGURE 1: PP2A binds to the C terminus of $\alpha_1$1.2 immediately distal to serine 1928. (A) Topology of the $\alpha_1$1.2 C terminus depicting the relative positions of serine 1928, the regions covered by the various $\alpha_1$1.2 GST-fusion proteins, and the stop-5, -6, -7, and -8 termination mutations. The two regions consistently seen to interact with PP2A/C are depicted with gray boxes; the region highlighted by the darker gray box was found to interact more strongly than the lighter gray region. (B) PP2A from the brain binds downstream of serine 1928. GST-fusion proteins of the C terminus of $\alpha_1$1.2 were immobilized and incubated with cytosol. Proteins present after washing and extraction were detected via immunoblotting with antibodies against PP2A/C (middle panel) and PP2A/A (top panel), followed by probing with the anti-GST antibody to determine relative amounts of fusion proteins present during the interaction assay (bottom panel). (C) Catalytic subunit of PP2A itself binds directly to $\alpha_1$1.2 downstream of serine 1928. Bacterial lysates containing expressed 6×His-tagged PP2A/C were incubated with the purified $\alpha_1$1.2 C-terminal GST-fusion proteins and detected by immunoblotting. The level and integrity of the GST-fusion proteins were in this experiment analyzed by Coomassie staining of a duplicate gel (bottom panel). Note the relatively stronger interaction signal for GST-CT-D, which contains the region just distal to serine 1928, despite the low abundance of GST-CT-D compared to the other GST-fusion proteins. Expected full-length GST-fusion proteins are indicated with arrowheads. Accordingly, GST-CT-D was degraded in B by ~6 kDa, and GST-CT-8 was degraded typically by 2−3 kDa. Similar results were obtained in multiple other experiments.

Zamponi, G. W., and Davis, M. J. Integrin receptor activation triggers converging regulation of $Ca_v1.2$ calcium channels by src and PKA pathways. *J. Biol. Chem.*, manuscript submitted). Culturing and transfection of tsA-201 cells was conducted as described in detail by us previously (*48*). Briefly, cells were maintained at 37 °C (5% CO_2) in Dulbecco's modified Eagle medium (DMEM), supplemented with fetal bovine serum, penicillin, and streptomycin. Cells were transfected with either wild type or truncated $\alpha_1$1.2, β_{1b}, and α_2-δ_1 and EGFP using the calcium phosphate method (*49*). In each case, 7 μg of each calcium channel subunit cDNA plus 1 μg of EGFP cDNA were used for transfection. The tsA-201 cells were moved to 28 °C at 24 h post-transfection and maintained for up to 3 days before electrophysiological or biochemical characterization.

Immunoprecipitation and Immunoblotting from tsA-201 Cells. For immunoprecipitation, the tsA-201 cells were trypsinized, resuspended in 5 mL phosphate-buffered saline, and centrifuged at 2000 rpm in a tabletop centrifuge. The pellet was flash frozen in liquid nitrogen and stored at −80 °C. For immunoprecipitation, cells were extracted with Triton X-100 solubilization buffer supplemented with phosphatase inhibitors (50 mM NaF, 20 mM Na pyrophosphate, 1 mM *p*-nitrophenyl phosphate, and 2 μM microcystin-LR). Lysates were cleared by ultracentrifugation and incubated for 3−4 h with anti-$\alpha_1$1.2 or nonspecific control antibodies and protein-A Sepharose before washing with phosphatase inhibitors (50 mM NaF, 20 mM Na pyrophosphate, and 1 mM *p*-nitrophenyl phosphate was added to the wash buffer) and immunoblotting as described above for brain extracts. Immunoblot signals were densitometrically quantified as described above for GST-CT-4. The ratio of the anti-$\alpha_1$1.2-P signal to the total anti-$\alpha_1$1.2 signal was determined for each sample. The ratios for stop 6 were normalized to the ratios of full-length $\alpha_1$1.2 within each experiment to allow for a comparison between experiments. Statistical analysis was performed as before.

Electrophysiology. Whole-cell patch-clamp recordings were conducted with an external solution containing (in millimolars) 20 $BaCl_2$, 1 $MgCl_2$, 10 HEPES, 40 tetraethylammonium chloride, 10 glucose, and 65 CsCl at pH 7.2. The pipet solution contained (in millimolars) 108 $CsCH_3SO_4$, 4 $MgCl_2$, 9 EGTA, and 9 HEPES at pH 7.2. Pipets had typical resistances of 3−4 MΩ. Series resistance was compensated by 85%. Data were acquired and filtered at 1 kHz with an Axopatch 200B amplifier, linked to a personal computer equipped with pCLAMP 9.0 software (Axon Instruments). I−V relations were fitted with the equation

$$I_{peak} = (V - E_{rev})G_{max}(1/(1 + \exp(V_{1/2,act} - V)/k_{act}))$$

where E_{rev} is the reversal potential, $V_{1/2,act}$ is the half-activation potential, G_{max} is the maximum slope conductance, and k_{act} is the slope factor. For display purposes, I−V curves were normalized to the maximum peak current amplitude to facilitate the comparison.

RESULTS

PP2A/C Binds Downstream of Serine 1928 in $\alpha_1$1.2. The catalytic subunit of PP2A (PP2A/C) binds directly to the C terminus of $\alpha_1$1.2 (*19*). Binding sites were further defined with recombinant purified GST-fusion proteins of various $\alpha_1$1.2 C-terminal sequences (Figure 1A). Incubation of these GST-fusion proteins with brain homogenate as a source of native PP2A and subsequent immunoblotting revealed that PP2A/C bound preferentially to CT-4, CT-8, and CT-D (Figure 1B). The original subcellular localization of PP2A/C did not matter because cytosolic and detergent-soluble

membrane fractions showed similar results (data not shown). All three fusion constructs contain residues 1944−2029 of the rabbit $\alpha_1$1.2 C terminus (1914−1999 of the rat sequence) just downstream of the PKA phosphorylation site of $\alpha_1$1.2 (serine 1928 in rabbit or serine 1898 in the shorter rat sequence). PP2A/C also consistently bound to CT-B upstream of serine 1928. However, this interaction was less robust than binding to CT-D/-4/-8 and CT-23 more often than not failing to bind to PP2A/C, although it contains the entire CT-B region (see below, Figure 1C).

Using brain homogenate for pull-down experiments of PP2A/C does not indicate whether the observed interactions are direct or mediated by other proteins in the brain extracts. The scaffolding A or perhaps one of the regulatory B/B′/B″ subunits of PP2A or other adapter-like proteins could serve to bridge the catalytic PP2A subunit to $\alpha_1$1.2. In fact, when we reprobed these immunoblots for the scaffolding PP2A/A subunit, which is a constitutive partner for PP2A/C in the majority of native PP2A complexes, we found the same binding pattern as for PP2A/C (Figure 1B). To address the issue of direct binding, we performed analogous binding assays using bacterially expressed 6×His-tagged PP2A/C (Figure 1C). PP2A/C again bound reproducibly the CT-4, CT-8, and CT-D as well as the CT-B and CT-23 fusion proteins. These results demonstrate clearly that PP2A/C binds in the absence of any other known PP2A scaffolding or targeting subunits to the CT-D and CT-B region. However, CT-D constitutes a much stronger binding site for PP2A/C than CT-B because a much smaller amount of CT-D pulls down PP2A/C to a similar degree as compared to CT-B (compare respective signals in top and bottom panels of Figure 1C). Similarly, binding of 6×His-PP2A/C to GST-CT-1 was weaker than to CT-D when considering the amount of GST-fusion protein present (Figure 1C) and was not observed with the brain extract (Figure 1B).

Careful inspection of the anti-GST signals and Coomassie-staining patterns throughout our experiments, which reflect the composition of each affinity-purified GST-fusion protein, shows that CT-D and CT-8 are in most experiments degraded. Especially revealing are experiments such as that illustrated in Figure 1B, in which the largest visible CT-D band ran with an apparent M_R of ~35 000 rather than the expected 41 000 (compare with CT-D in Figure 1C). In this case, CT-D was obviously missing about 50 residues at its C terminus yet still bound strongly to PP2A. In other experiments, CT-D of the size expected for its full-length form was observed (e.g., Figure 1C), albeit at lower expression levels. CT-8 also typically showed a truncation of about 20 residues at its C terminus (parts B and C of Figure 1). It is possible that the region around residue 2000 is specifically sensitive to proteolytic cleavage in these fragments. Full-length CT-D and CT-8 contain residues 1944−2067 and 1909−2029 of rabbit $\alpha_1$1.2. Because CT-D was truncated by about 50 residues and CT-8 by about 20 residues, these binding assays narrow down a core sequence of residues 1944−2000 for PP2A/C binding. Furthermore, CT-C (residues 1834−1957 in rabbit $\alpha_1$1.2) did not interact with PP2A/C; hence, these residues are not necessary for PP2A/C association. These considerations indicate that the segment defined by residues from 1958 to about 2000 is crucial for PP2A/C binding to this region.

PP2A Is the Main Serine 1928 Phosphatase. We have shown earlier that PP2A that co-immunoprecipitates with $\alpha_1$1.2 C can dephosphorylate serine 1928 (*19*). To test whether PP2A is the principal serine 1928 phosphatase in the brain, GST-CT-4 was immobilized on glutathione Sepharose, phosphorylated *in vitro* by the purified PKA catalytic subunit, and incubated with aliquots of brain cytosol that had been pretreated with various phosphatase inhibitors. The level of phosphorylated serine 1928 remaining after the dephosphorylation reactions was assessed via immunoblotting with our phosphospecific antibody against this site, followed by stripping the blots and probing with anti-GST. The ratio of the anti-$\alpha_1$1.2-P immunosignal to the anti-GST immunosignal was determined for each sample to facilitate the comparison between samples. The ratios were normalized to the input ratio, thus allowing for a comparison between experiments. Figure 2A shows a representative immunoblot of one of these experiments in which increasing concentrations of okadaic acid and fostriecin was used to inhibit dephosphorylation. The addition of cytosol without inhibitors resulted in dephosphorylation of serine 1928 of phosphorylated CT-4 (compare lane 2 with lane 1; the sample in lane 1 was not treated with cytosol). Okadaic acid (5 and 50 nM, lanes 4 and 5) and microcystin (50 nM) significantly inhibited dephosphorylation (parts A and B of Figure 2). These results point toward PP2A as the relevant phosphatase because its activity is blocked by these inhibitors at these concentrations in contrast to the activities of the other two main phosphatases, PP1 and PP2B (*50*, *51*). To ensure that immunosignals were in the linear range, increasing amounts of GST were analyzed by immunoblotting and ECL signals were quantified (Figure 2C). Within the range used for quantification, doubling the amount of GST or doubling the exposure time increased the signal by about 2-fold and compared well to the signal-scanned signal via Coomassie staining. The analogous analysis that defines the linear range for our anti-$\alpha_1$1.2 and anti-$\alpha_1$1.2-P antibodies was published earlier (*20*).

To further differentiate between PP2A and PP1, which may also be significantly inhibited by okadaic acid (IC_{50} = 20 nM) and microcystin (IC_{50} = 0.2 nM) at these concentrations, we tested the effects of inhibitor 2, a highly specific endogenous PP1 inhibitor (*52*), with negative results. Furthermore, fostriecin, a selective PP2A inhibitor, resulted in a concentration-dependent inhibition of dephosphorylation (lanes 6−11 of Figure 2A), with 500 nM fostriecin effectively blocking the dephosphorylation. This concentration is far below the IC_{50} for PP1 inhibition, which is at or above 45 μM (*50*, *51*, *53*).

Because PP2B, the only other main serine/threonine phosphatase besides PP1 and PP2A, has a very low sensitivity toward okadaic acid and microcystin, it seems an unlikely candidate for dephosphorylating serine 1928 based on the microcystin, okadaic acid, and fostriecin effects. Nevertheless, we tested two different PP2B-selective inhibitors, cyclosporine and cypermethrin (*51*, *54*), but observed no effect (Figure 2B). In consideration of the PP2B activity, we did not include EDTA and EGTA during the homogenization procedures to not chelate Ca^{2+}. We regularly determine Ca^{2+} levels in our buffers, which are between 2 and 3 μM (*55*), severalfold higher than the K_d value of PP2B for Ca^{2+}, which has a high affinity for Ca^{2+} (*56*, *57*). In addition, Ca^{2+} levels are substantial in brain homogenate and sufficient

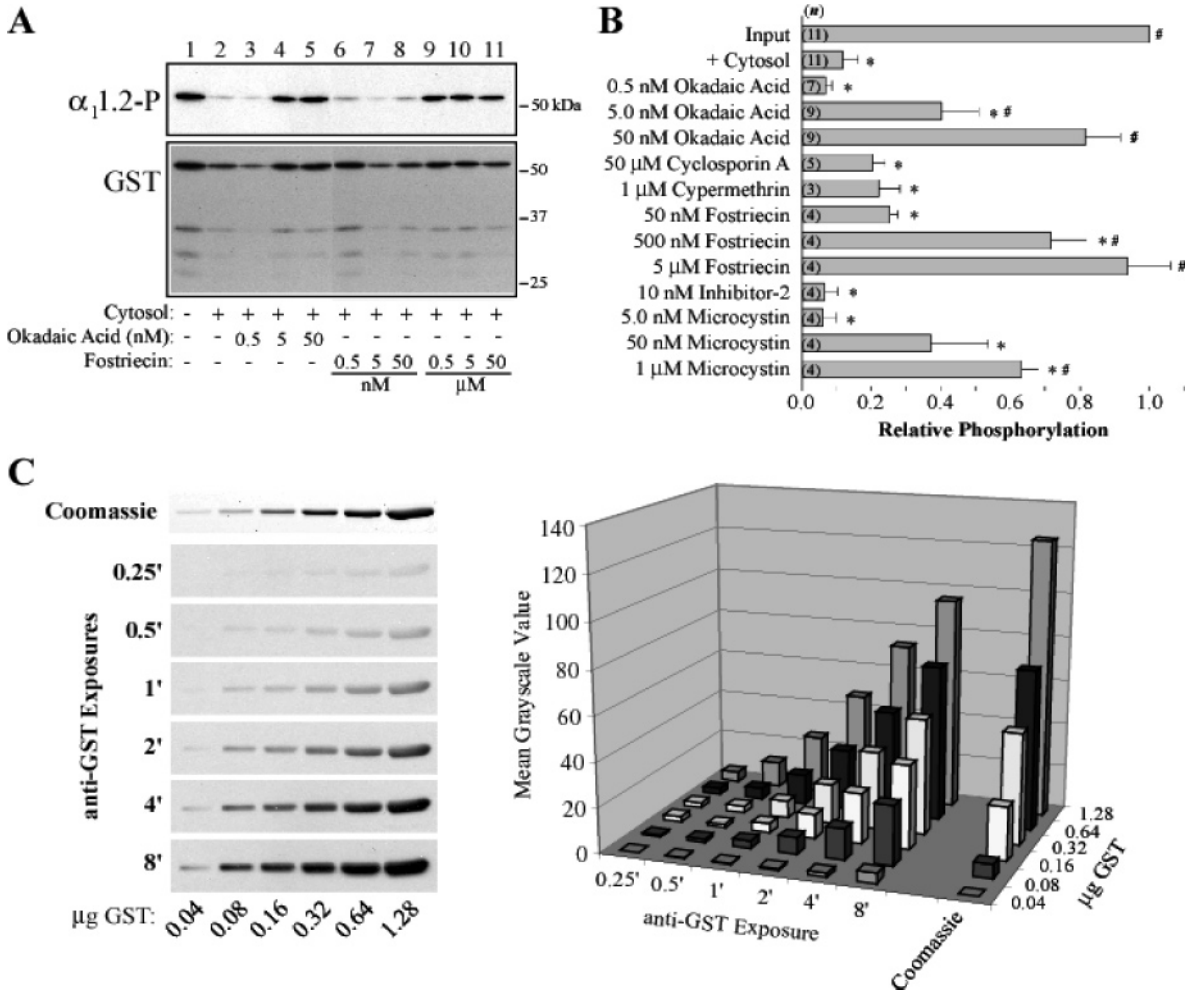

FIGURE 2: Inhibitors of PP2A but not other phosphatases prevent dephosphorylation of serine 1928 during incubation with brain lysate. GST-CT-4 was immobilized and incubated with purified PKA and Mg^{2+}-ATP to phosphorylated serine 1928. Brain cytosol was preincubated with or without the indicated phosphatase inhibitors for 30 min before the addition to GST-CT-4 for 45 min at 37 °C. The sample in lane 1 did not receive any cytosol. GST-CT-4 was analyzed by immunoblotting with the phosphospecific antibody $\alpha_1$1.2-P against phosphorylated serine 1928, followed by reprobing with the anti-GST antibody. (A) Okadaic acid and fostriecin inhibit dephosphorylation of GST-CT-4. (B) Summary of dephosphorylation assays. The ratio of the anti-$\alpha_1$1.2-P signal to the anti-GST signal on immunoblots via densitometry was normalized to the initial starting level of phosphorylated GST-CT-4 in each experiment ("Input"), which was treated in the absence of cytosol. The number of experiments for each bar is indicated in parentheses. (*) $p < 0.05$ in comparison to Input; (#) $p < 0.05$ in comparison to + Cytosol. (C) Linearity of ECL signals. The concentration of GST was determined by Bradford and bicinchoninic acid protein assays, which yielded equal results. Increasing amounts of GST were loaded for SDS−PAGE, followed by immunoblotting with anti-GST and film exposure for increasing time intervals, as indicated on the left (in minutes). ECL signals were quantified by densitometry for all time points and concentrations (right panel). A parallel SDS−PAGE experiment was stained with Coomassie (top left panel).

to fully activate PP2B as long as chelators are not added (*56*, *57*).

By themselves, these phosphatase inhibition studies argue against PP1 and PP2B as major serine 1928 phosphatases and strongly imply PP2A activity. The concentrations at which okadaic acid, microcystin, and fostriecin inhibited serine 1928 dephosphorylation in our hands were higher than expected from reported IC_{50} values of these drugs for PP2A (0.1, 0.2, and 3 nM, respectively) (*50*). These values were determined using purified enzymes. Because we used cytosol as a source for endogenous PP2A, it is likely that there are significant specific and nonspecific interactions of the inhibitors with other phosphatases and other constituents in our dephosphorylation assays, including tube walls. Instability is an added problem especially for fostriecin, which has a half-life of less than 30 min in aqueous solutions.

To further address the question of which phosphatases are able to dephosphorylate serine 1928, PP1, PP2A, PP2B, and PP5 were immunoprecipitated. In parallel, affinity-purified GST-CT-4 was phosphorylated with PKA similar to those experiments described in Figure 2, except that the GST-CT-4 was kept in solution and not immobilized. To initiate dephosphorylation, aliquots of phosphorylated GST-CT-4 were added to the different phosphatase immunoprecipitates, which remained on the protein A beads. The different samples were incubated for 3−30 min under agitation to prevent the beads from settling. Incubations with immunoprecipitated PP2A/C led to rapid dephosphorylation of CT-4. However, immunoprecipitated PP1, PP5, and PP2B were not able to dephosphorylate CT-4 (Figure 3). PP2A therefore appears to be the phosphatase that is mainly responsible for dephosphorylating serine 1928. To further scrutinize a contribution by PP1 or PP2B to serine 1928 dephopshorylation, we incubated phosphporylated GST-CT-4 with what is considered a large amount of purified PP1 and PP2B, following protocols by GloboZymes, the

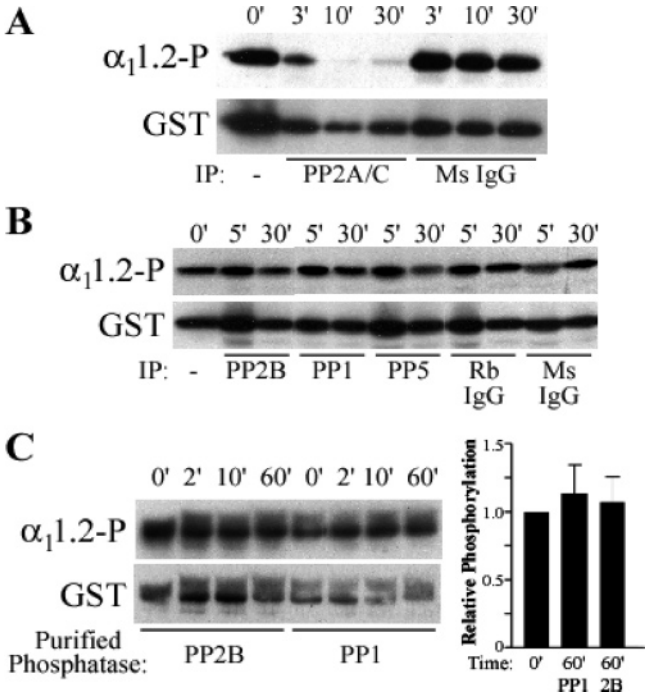

FIGURE 3: PP2A/C but not other phosphatases from the brain dephosphorylate serine 1928 *in vitro*. PP2A (A) or PP1, PP2B, and PP5 (B) were immunoprecipitated from the cytosolic fraction from rat brain using the respective antibodies (see the Experimental Procedures). Purified nonspecific mouse or rabbit IgG (Ms IgG and Rb IgG, respectively) were used for control immunoprecipitations. Phosphorylated GST-CT-4 was incubated with the immunoprecipitates or 0.05 units/sample highly purified PP1 or PP2B from GloboZymes for the indicated times at 37 °C. Dephosphorylation was stopped by extraction with SDS sample buffer for 5 min at 90 °C. The 0′ time point represents the initial phosphorylation level of GST-CT-4 before the addition to phosphatases. Immunoblots were probed with anti-$\alpha_1$1.2-P followed by anti-GST. Phosphorylation levels were quantified for the purified phosphatases (C, right) as in Figure 2 and were found to be insignificant ($p < 0.05$, *t* test).

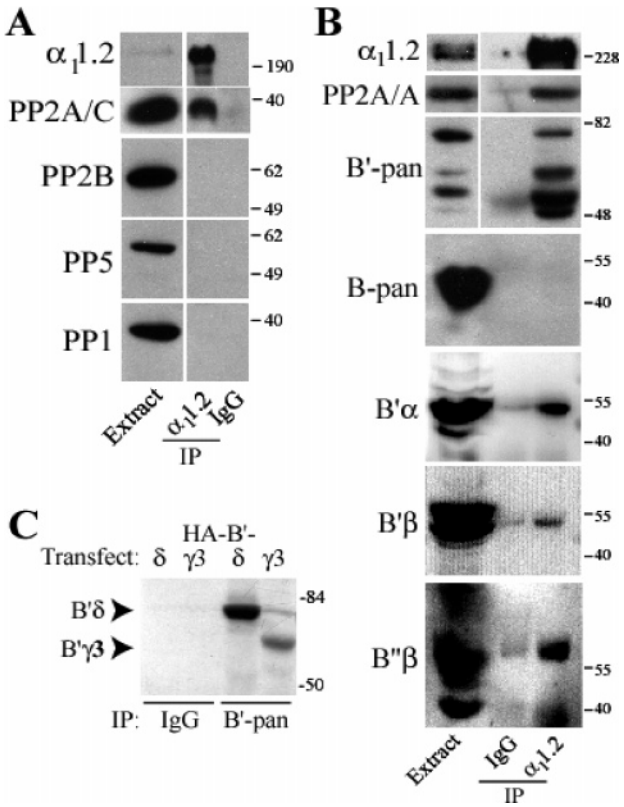

FIGURE 4: PP2A/C, PP2A/A, PP2A/B′, and PP2A/B″ but not PP2A/B, PP1, PP2B, or PP5 coimmunoprecipitate with $\alpha_1$1.2. Rat cortical lysates (A and B) and HEK293 cell extracts (C) were used for immunoblotting either directly ("Extract") or after solubiliztion of the membrane fraction followed by immunoprecipitation. (A) Ca_v1.2 was immunoprecipitated with anti-$\alpha_1$1.2 before immunoblotting with antibodies against PP2A/C, PP2B, PP5, and a pan-specific antibody against all known PP1 isoforms. Extract lanes were loaded as positive controls for the detection of the respective phosphatase during the immunoblotting. (B) Immunoblotting of cortical lysates and $\alpha_1$1.2 immunoprecipitates with antibodies specific for different PP2A subunits including anti-PP2A/A, anti-B′-pan, anti-B-pan, which recognizes all three B subunit isoforms (*43*), anti-B′α, anti-B′*β*, and anti-B″*β* (PR59), as indicated. The anti-B′-pan recognizes four bands in the extract, as expected because of the presence of four isoforms in the expected molecular range. All known B subunit isoforms have similar molecular masses and comigrate in a single band as illustrated by the extract lane. As a control for the specificity of the immunoprecipitations, nonspecific rabbit IgG was used in parallel with anti-$\alpha_1$1.2. All three lanes in the top three panels were rearranged to eliminate nonrelevant lanes. (C) Characterization of the anti-B′-pan antibody. Our pan-specific B′ antibody (anti-B′-pan) detected both, HA-tagged rabbit B′γ3 and B′δ subunits ectopically expressed in HEK 293 cells when used for immunoprecipitation followed by immunoblotting.

distributor. No dephosphorylation was observed (Figure 3C).

To further characterize putative interactions of native $\alpha_1$1.2 with the various phosphatases, we immunoprecipitated $\alpha_1$1.2 from Triton X-100, solubilized membranes, and examined the presence of different phosphatases in the Ca_v1.2 immune complexes (Figure 4). We found earlier that PP2A but not PP1γ, which is one of the three isoforms of PP1, nor PP2B coimmunoprecipitated with $\alpha_1$1.2 under our conditions (*19*) and have since confirmed these results in multiple experiments over the past 5 years (Figure 4A). We extended these experiments to include PP1α and PP1δ, the other two PP1 isoform besides PP1γ, and PP5 in our analysis (Figure 4A). Neither the PP1 nor the PP5 antibody detected a band in the Ca_v1.2 complex after immunoprecipitation under our conditions. The PP1 antibody in these experiments recognizes all PP1 isoforms (*39*); hence, the negative result with respect to this antibody suggests that none of the PP1 isoforms was present in these Ca_v1.2 immunoprecipitates.

PP2A typically exists as a trimeric holoenzyme that contains the catalytic C, a structural A, and a targeting regulatory subunit (*51*, *58*−*60*). More than 15 PP2A regulatory subunits are known, which are subdivided into three classes (B, B′, and B″) (*34*, *58*, *60*, *61*). The substrate specificity of a trimeric PP2A holoenzyme is often determined by the targeting B/B′/B″ subunit in the complex (*58*). Although binding of PP2A to Ca_v1.2 is mediated by a direct interaction of PP2A/C with $\alpha_1$1.2 (Figure 1C), targeting B/B′/B″ subunits may still play a role in docking PP2A at this channel. In fact, immunoprecipitation of $\alpha_1$1.2 led to coprecipitation of various B′ and B″ subunits, but B subunits were not detectable, as detailed below (Figure 4B).

Our pan-specific antibody against the middle region of B′δ, which is conserved among B′ subunits, recognizes a total of four bands in the homogenate of the rat brain cortex, most likely corresponding to the four different B′ isoforms (B′α−δ), which are encoded by four different genes (see Figure 4B, B′-pan, extract lane). To confirm that our pan-B′ antibody interacts not only with B′δ but also with other B′

subunits, we expressed B′γ3 in HEK293 cell cultures in parallel with B′δ. B′γ3 is one of several splice forms of B′γ, which differ only by minor alterations at their C termini (*34*, *61*). Using the pan-B′ antibody for immunoprecipitation from these cultures and subsequent immunoblotting resulted in the detection of both B′ isoforms (Figure 4C). All four bands detected by the pan-B′ antibody in the total brain extract were also present in the $Ca_v1.2$ immune complexes but not in control immunoprecipitates (Figure 4B). These results indicate that PP2A holoenzymes containing any of the four B′ subunits can associate with $Ca_v1.2$. This conclusion was further confirmed with subtype-specific antibodies against B′α and B′β. Both isoforms specifically coimmunoprecipitated with $Ca_v1.2$ (middle panels of Figure 4B). B″ subunits share structural features with B′ subunits that are thought to determine PP2A targeting. Similar to B′ subunits, the B″β subunit typically called PR59 also coimmunoprecipitated with $Ca_v1.2$ in a specific fashion (bottom panel of Figure 4B). In addition to B′ and B″ subunits, four different B-type subunits, B$\alpha-\delta$, exist. The structures of the B subunits are very different from those of B′ and B″ subunits. These four isoforms have nearly identical molecular masses and comigrate as a single band during SDS−PAGE, as illustrated in the lysate lane in Figure 4B. No such band was detectable following $Ca_v1.2$ immunoprecipitation, indicating that $Ca_v1.2$ does not interact with PP2A holoenzymes containing Bα, β, γ, or δ under our conditions (top panel in Figure 4E).

Dephosphorylation of Serine 1928 Depends upon the PP2A/C Binding Site Downstream of Serine 1928. Constitutive anchoring of kinases and phosphatases at substrate proteins is often critical for their effective phosphorylation and dephosphorylation (*25*−*27*). Therefore, we tested whether docking of PP2A to the segment immediately downstream of serine 1928 is crucial for its effective dephosphorylation in intact cells. We expressed truncation mutants of $\alpha_1$1.2 (stop 5−stop 8) in HEK293-derived tsA-201 cells along with the β_{1b} and α_2-δ_1 subunits (Figure 5). The relative positions of the truncations for stop 5−stop 8 of the rabbit sequence are 1889, 1956, 2026, and 2093 (Figure 1A). Under basal conditions, serine 1928 phosphorylation is relatively low yet clearly measurable: 16.7% of $\alpha_1$1.2 is phosphorylated in the rat brain, reflecting a basal activity of PKA (*20*). If dephosphorylation is inhibited by removing the PP2A binding site downstream of serine 1928, basal phosphorylation should be increased. After the cells were harvested and homogenized with phosphatase inhibitors, we immunoprecipitated $\alpha_1$1.2 and monitored serine 1928 phosphorylation levels with the anti-$\alpha_1$1.2-P phosphospecific antibody. We reprobed these immunoblots for the amount of total $\alpha_1$1.2 with the same antibody used for immunoprecipitation. The endogenous phosphorylation level of stop 6 is dramatically higher than the phosphorylation level of full-length wild-type $\alpha_1$1.2 (parts A and B of Figure 5). It is also clearly higher than that of stop 7 or stop 8 (Figure 5C). Stop 5 does not contain serine 1928, hence, the expected lack of anti-$\alpha_1$1.2-P immunoreactivity. Total amounts of anti-$\alpha_1$1.2-P immunoprecipitated from each culture were comparable. Truncating anti-$\alpha_1$1.2-P from stop 7 to stop 6 approximates the loss of the 1958−2000 binding site and supports the idea that this region is necessary for proper regulation of serine 1928 phosphorylation.

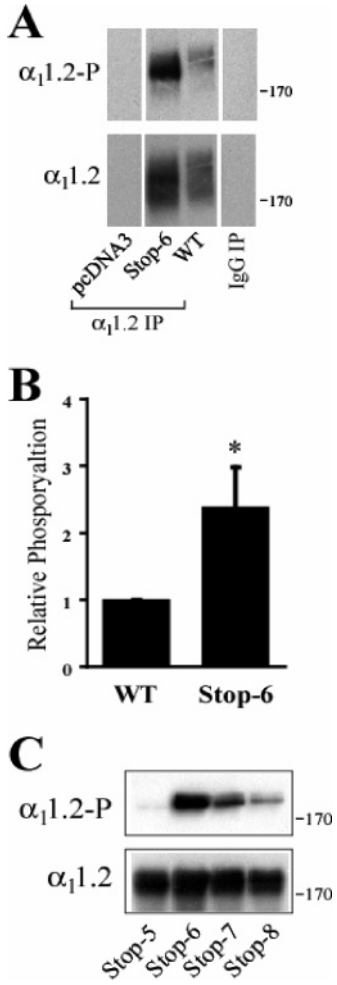

FIGURE 5: Truncation of the major PP2A/C binding site on $\alpha_1$1.2 results in higher basal serine 1928 phosphorylation in intact cells. Cultures of tsA-201 cells were transfected with wild-type $\alpha_1$1.2 (WT) or the indicated $\alpha_1$1.2 truncation mutants stop 5−8, along with β_{1b} and α_2-δ_1 subunits, or plain pcDNA3 vector, as a negative control. Cells were extracted with Triton X-100 for immunoprecipitation with anti-$\alpha_1$1.2 or nonspecific control IgG (from WT transfected cells). Immunoblots of the immunocomplexes were probed with the phosphospecific anti-$\alpha_1$1.2-P antibody followed by stripping and reprobing for total $\alpha_1$1.2 with the anti-$\alpha_1$1.2 antibody. Stop-6 in which the PP2A binding site downstream of serine 1928 had been deleted consistently showed a higher phosphorylation level than the WT (A and B) and stop-7 or -8 (C). The ratio of the anti-$\alpha_1$1.2-P signal to the anti-$\alpha_1$1.2 signal was quantified from four independent experiments via densitometry and normalized by setting the WT ratio equal to 1. The difference in the phosphorylation ratios was statistically significant ($p < 0.05$; *t* test). All four lanes in A were from the same exposure but rearranged to eliminate nonrelevant lanes.

To ensure that all stop mutants were functionally and structurally intact and present at the cell surface and therefore equally available for phosphorylation and dephosphorylation, tsA-201 cells were transfected with $\alpha_1$1.2, α_2-δ_1, and β_{1b} as for the analysis of serine 1928 phosphorylation in intact cells. All of the channels yielded robust whole-cell currents with maximum slope conductances ranging from 15 nS (stop 5) to 28 nS (stop 8). The currents displayed similar activation and inactivation kinetics with the exception of stop 5, which displayed a slightly more rapid time course of inactivation. Accordingly, all of the mutant channel constructs supported the functional cell surface expression of $Ca_v1.2$ channels that display the expected functional characteristics. Figure 6

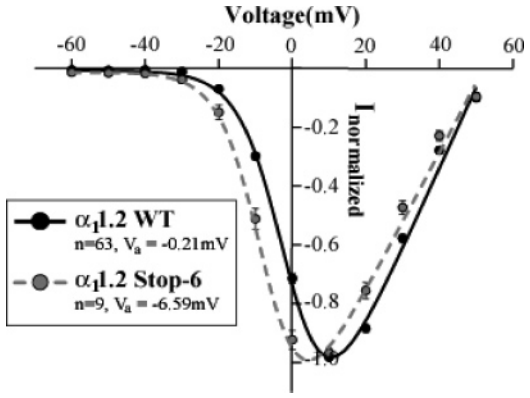

FIGURE 6: Ensembles of whole-cell I−V relations for WT and stop-6 $\alpha_1$1.2 in tsA-201 cells. Cultures were transfected with WT $\alpha_1$1.2 or stop 6 together with β_{1b} and α_2-δ_1. Truncation of $\alpha_1$1.2 at the stop-6 position (and also the other stop positions, not shown) resulted in effective surface expression of functional Ca_v1.2. The two I−V relations were normalized to a peak current amplitude of 1.0 to facilitate the comparison. Error bars denote standard errors, and the solid and dashed lines reflect fits to the Boltzmann equation for WT and stop 6, respectively. The half-activation potentials obtained from the fits are indicated (V_a). The difference between V_a for WT and stop 6 was statistically significant ($p < 0.05$; ANOVA).

shows ensembles of the current−voltage ($I-V$) relations acquired from cells expressing either wild type or stop 6 $\alpha_1$1.2. Currents were normalized with the peak current set equal to 1 to facilitate the comparison of the two curves. As evident from Figure 6, the half-activation potentials observed with the mutant channels were approximately 6 mV more hyperpolarized compared to that of the wild-type channel. Such a left-shift in the $I-V$ curve would be expected if PKA-mediated phosphorylation is increased.

DISCUSSION

Excision of inside-out patches from rabbit ventricular myocytes leads to the run-down of L-type channel currents that can be inhibited by okadaic acid and reversed by PKA (*33*). These findings suggest that a phosphatase must be docked near or at the channel that counteracts upregulation of Ca_v1.2 by PKA. A number of additional findings indicate that PP2A and in some cases also PP1 can reverse PKA-mediated phosphorylation of Ca_v1.2 (*51*). Injection of purified PP2A and also PP1 reduces whole-cell L-type currents in guinea pig and rat cardiomyocytes following their upregulated by β-adrenergic stimulation via PKA (*62*). Neither phosphatase reduced basal currents in these cases. PP1/PP2A blockers also reverse or occlude PKA-mediated increases in L-type currents in the frog heart (*63*, *64*). Our previous results indicate that PP2A is stably bound to about 80% of Ca_v1.2 in the rat forebrain (*19*). The remainder of the Ca_v1.2 complexes that lack PP2A may represent an intracellular channel pool that may not bind as effectively to PP2A. These findings suggested that constitutive association of PP2A with Ca_v1.2 is critical for the regulation of Ca_v1.2 by PP2A. We now show that the main PP2A binding site on $\alpha_1$1.2 resides immediately downstream of serine 1928 (Figure 1), the most prevalent if not only PKA phosphorylation site on $\alpha_1$1.2 (*11*, *16*−*21*). Our *in vitro* dephosphorylation studies with various phosphatase inhibitors and purified phosphatases further point toward PP2A as the main phosphatase for dephosphorylation of serine 1928 (Figures 2 and 3). In fact, PP2A is the only phosphatase that is detectable in Ca_v1.2 immunoprecipitates by subsequent immunoblotting under our conditions (Figure 4). Finally, truncation of residues downstream of serine 1928 increases the phosphorylation level of serine 1928 in intact cells (Figure 5). Our results suggest that PP2A binding to a region covering residues from 1958 to about 2000 (Figure 1) is critical for effective dephosphorylation of serine 1928 (Figure 5) and thereby for the regulation of channel activity (Figure 6).

PKA has to be docked via AKAPs (*25*, *65*) at certain substrates such as AMPA-type glutamate receptors (*28*) and the L-type channels Ca_v1.1 and Ca_v1.2 (*21*, *29*) for their efficient phosphorylation. For dynamic control of the functions of these ion channels and of a number of other effectors, phosphorylation must be counteracted by dephosphorylation. However, only a few studies have shown that docking of phosphatases at or near their substrates is as crucial for dephosphorylation as kinase anchoring for phosphorylation. PP1 is linked to the AMPA-type glutamate receptors by spinophilin (*66*) and to NMDA-type glutamate receptors through yotiao, which also servers as an AKAP (*67*). PP2A has been found to interact with the β_2 adrenergic receptor (*68*) and to Ca^{2+}- and calmodulin-dependent kinase IV (*69*). Spinophilin also targets PP1 to the cardiac ryanodine receptor type 2 via a leucine/isoleucine zipper (LZ) interaction (*70*). The type-2 ryanodine receptor is precisely juxtaposed to Ca_v1.2 in cardiomyocytes for reliable excitation−contraction coupling. Although some evidence indicates that PP1 regulates Ca_v1.2 in the heart (*51*), none of the PP1 isoforms nor any of their know adaptor proteins including yotiao, neurabin, spinophilin, AKAP149, and AKAP220 have been reported to interact with Ca_v1.2. We did not detect PP1 in the Ca_v1.2 complex from the brain or heart in multiple experiments over several years using different PP1 antibodies (*19*) (Figure 4 and data not shown). It is conceivable that PP1 that is docked at a neighboring protein, perhaps the ryanodine receptor, could act on nearby Ca_v1.2. Alternatively, PP1 may not have to be anchored in the case of Ca_v1.2. Also, serine 1928 was not effectively dephosphorylated by highly purified PP1, in contrast to its dephosphorylation by PP2A (Figure 3). If PP1 controls Ca_v1.2 activity, it might do so by dephosphorylating other sites that might be targeted by kinases different from PKA.

PP2A is also intimately associated with a number of its substrates, including the β_2 adrenergic receptor (*68*), CaMKIV (*69*), and the type-2 ryanodine receptor (*70*). Typically, the substrate specificity of PP2A is at least in part determined by the targeting B/B′/B″ subunit in the trimeric holoenzyme (*58*). The B″ subunit PR130 (*71*) links PP2A to the type-2 ryanodine receptor via a second LZ interaction that is different from the one that binds PP1 (*70*). However, a third LZ of the ryanodine receptor binds to mAKAP for PKA anchoring (*70*). Despite the close proximity of the ryanodine receptor and Ca_v1.2, both channels associate themselves with PKA and PP2A. Obviously, mere proximity is not sufficient to allow for the sharing of anchored PKA or PP2A. It is also conceivable that these two enzymes have to be arranged in a specific conformation to ensure fast and efficient phosphorylation and dephosphorylation, respectively. Our finding that PP2A binding immediately downstream of serine 1928 is in this respect notable because this interaction could foster a favorable spatial arrangement between the catalytic

site of PP2A and its substrate to ensure quick and unhindered dephosphorylation of serine 1928.

In the trimeric holoenzyme, regulatory B/B′/B″ subunits typically have the role of targeting PP2A to different subcellular domains and specific proteins, thereby determining substrate specificity (*58*). More than 15 regulatory B, B′, and B″ subunits are known (*34*, *58*, *60*, *61*). As mentioned above, the B″ subunit PR130 (*71*) mediates PP2A binding to the type-2 ryanodine receptor. The interaction of PP2A with $Ca_v1.2$, however, relies on the direct association of the PP2A/C subunit with $\alpha_1 1.2$ because bacterially expressed PP2A/C and $\alpha_1 1.2$ fragments bind to each other (Figure 1C). It is, therefore, not surprising that multiple targeting regulatory subunits of PP2A including all four B′ isoforms and at least one B″ isoform (i.e., PR59) copurify with $Ca_v1.2$ (Figure 4B). In addition to the gene for the B″ subunit PR59, two other genes are known to encode B″ subunits (*60*). PR72 and PR130 originate from the same gene by differential splicing, and PR48 is encoded by the third B″ gene. We have not tested whether one of the other B″ subunits are also present in the $Ca_v1.2$ complex, but this possibility does not seem unlikely given the similarities between B″ subunits (>60% identity between isoforms).

Remarkable is the apparent lack of any of the four B$\alpha-\delta$ subunits in the PP2A−$Ca_v1.2$ complex (Figure 4E). B′- and B″-family subunits are structurally more related to each other than to B-family subunits. B-family subunits are mostly β-sheet structure containing proteins predicted to adopt a β-propeller fold (*72*), while B′- and B″-family subunits are composed mainly of α-helical repeats (Strack, S., unpublished observations). Binding of the heterotrimeric PP2A holoenzyme to $Ca_v1.2$ may be stabilized by secondary interactions with B′- and B″-family subunits, which may not be possible with the B-family isoforms. It is equally conceivable that B- but not B′- or B″-family subunits cause steric or allosteric interference of PP2A/C binding to $Ca_v1.2$. Such effects could be analogous to those of the PP1 adaptor protein, myosin phosphatase targeting protein 1 (MYPT1) (*73*). The increase in PP1δ activity toward the myosin light chain is due to the adaptor function of MYPT1 (*74*). Analogously, B′ and B″ subunits may increase the binding of the PP2A holoenzyme via secondary interactions with $Ca_v1.2$. MYPT1 also decreases PP1δ activity for substrates other than the myosin light chain by restricting substrate access to the catalytic site of PP1δ. Similarly, B but not B′ or B″ subunits may restrict access of $Ca_v1.2$ to PP2A/C.

$Ca_v1.2$ interacts not only with AKAP15/18 (*30*) as shown in the heart and the AKAP MAP2B in the brain (*18*) but also with AKAP150 (Davare, M. A., Hall, D. D., Shi, M., and Hell, J. W., unpublished results) and its human homologue AKAP79 (*31*). AKAP79/150 in turn binds PP2B in addition to PKA (*75*, *76*) and could recruit PP2B to the $Ca_v1.2$ complex. Nevertheless, we never observed PP2B in the immunoprecipitated $Ca_v1.2$ complex (e.g., Figure 4A) (*19*). Furthermore, PP2B-specific inhibitors typically do not affect L-type currents in the heart (*63*, *77*) or neurons (*78*). However, the situation may be different in smooth muscle cells, where evidence indicates that $Ca_v1.2$ activity is downregulated by PP2B (*79*).

Three different modes of channel activity have been distinguished for $Ca_v1.2$ (*80*). The channel is not available for activation in mode 0, shows short openings in mode 1, and long openings and short closings in mode 2 (*80*). Stimulation of the β-adrenergic receptor−PKA signaling pathway induces the transition from mode 0 to mode 1 or 2 (*13*, *81*). Okadaic acid blocks and the application of PP2A to excised inside-out membrane patches promotes the reversal of mode 2 and 1 in cardiac and smooth muscle cells (*82*−*84*). Collectively, these previous physiological results and our biochemical data indicate that PP2A reverses phosphorylation of serine 1928 and the ensuing upregulation of $Ca_v1.2$ activity by PKA only if anchored next to serine 1928. Hence, the exact localization of PP2A in the $Ca_v1.2$ channel complex is crucial for the correct physiological function of this L-type Ca^{2+} channel.

ACKNOWLEDGMENT

The authors thank Drs. S. Rossie, Purdue University, West Lafayette, IN, for providing the anti-PP5 antibody; J. W. Tracy, University of Wisconsin, Madison, WI, for providing the anti-GST antibody; D. M. Virshup, Huntsman Cancer Institute, University of Utah, Salt Lake City, UT, for the gift of the anti-B′α and anti-B′β antibodies; E. Ogris, Vienna Biocenter, Vienna, Austria, for the anti-B″ antibody; M. Marlene Hosey, Northwestern University, Chicago, IL, for the expression constructs for GST-CT-1, -CT-4, -CT-5, CT-7, -CT-8, -CT-14, and -CT-23; and T. P. Snutch, University of British Columbia, Vancouver, Canada, for providing the expression constructs for wild-type $\alpha_1 1.2$, rat β_{1b}, and rat α_2-δ_1.

REFERENCES

1. Catterall, W. A. (2000) Structure and regulation of voltage-gated Ca^{2+} channels, *Annu. Rev. Cell Dev. Biol. 16*, 521−555.
2. Hell, J. W., Westenbroek, R. E., Warner, C., Ahlijanian, M. K., Prystay, W., Gilbert, M. M., Snutch, T. P., and Catterall, W. A. (1993) Identification and differential subcellular localization of the neuronal class C and class D L-type calcium channel α1 subunits, *J. Cell Biol. 123*, 949−962.
3. Sinnegger-Brauns, M. J., Hetzenauer, A., Huber, I. G., Renstrom, E., Wietzorrek, G., Berjukov, S., Cavalli, M., Walter, D., Koschak, A., Waldschutz, R., Hering, S., Bova, S., Rorsman, P., Pongs, O., Singewald, N., and Striessnig, J. J. (2004) Isoform-specific regulation of mood behavior and pancreatic β cell and cardiovascular function by L-type Ca^{2+} channels, *J. Clin. Invest. 113*, 1430−1439.
4. Marrion, N. V., and Tavalin, S. T. (1998) Selective activation of Ca^{2+}-activated K^+ channels by co-localized Ca^{2+} channels in hippocampal neurons, *Nature 395*, 900−905.
5. Grover, L. M., and Teyler, T. J. (1990) Two components of long-term potentiation induced by different patterns of afferent activation, *Nature 347*, 477−479.
6. Bolshakov, V. Y., and Siegelbaum, S. A. (1994) Postsynaptic induction and presynaptic expression of hippocampal long-term depression, *Science 264*, 148−152.
7. Christie, B. R., Schexnayder, L. K., and Johnston, D. (1997) Contribution of voltage-gated Ca^{2+} channels to homosynaptic long-term depression in the CA1 region *in vitro*, *J. Neurophysiol. 77*, 1651−1655.
8. Wang, H. X., Gerkin, R. C., Nauen, D. W., and Bi, G. Q. (2005) Coactivation and timing-dependent integration of synaptic potentiation and depression, *Nat. Neurosci. 8*, 187−193.
9. Ghosh, A., and Greenberg, M. E. (1995) Calcium signaling in neurons: Molecular mechanisms and cellular consequences, *Science 268*, 239−247.
10. Dolmetsch, R. E., Pajvani, U., Fife, K., Spotts, J. M., and Greenberg, M. E. (2001) Signaling to the nucleus by an L-type calcium channel−calmodulin complex through the MAP kinase pathway, *Science 294*, 333−339.
11. De Jongh, K. S., Murphy, B. J., Colvin, A. A., Hell, J. W., Takahashi, M., and Catterall, W. A. (1996) Specific phosphorylation of a site in the full length form of the α1 subunit of the

cardiac L-type calcium channel by adenosine 3′,5′-cyclic monophosphate-dependent protein kinase, *Biochemistry 35*, 10392−10402.
12. Reuter, H. (1983) Calcium channel modulation by neurotransmitters, enzymes and drugs, *Nature 301*, 569−574.
13. Bean, B. P., Nowycky, M. C., and Tsien, R. W. (1984) β-Adrenergic modulation of calcium channels in frog ventricular heart cells, *Nature 307*, 371−375.
14. Sculptoreanu, A., Rotman, E., Takahashi, M., Scheuer, T., and Catterall, W. A. (1993) Voltage-dependent potentiation of the activity of cardiac L-type calcium channel α1 subunits due to phosphorylation by cAMP-dependent protein kinase, *Proc. Natl. Acad. Sci. U.S.A. 90*, 10135−10139.
15. Bunemann, M., Gerhardstein, B. L., Gao, T., and Hosey, M. M. (1999) Functional regulation of L-type calcium channels via protein kinase A-mediated phosphorylation of the β2 subunit, *J. Biol. Chem. 274*, 33851−33854.
16. Hell, J. W., Yokoyama, C. T., Breeze, L. J., Chavkin, C., and Catterall, W. A. (1995) Phosphorylation of presynaptic and postsynaptic calcium channels by cAMP-dependent protein kinase in hippocampal neurons, *EMBO J. 14*, 3036−3044.
17. Hell, J. W., Yokoyama, C. T., Wong, S. T., Warner, C., Snutch, T. P., and Catterall, W. A. (1993) Differential phosphorylation of two size forms of the neuronal class C L-type calcium channel α1 subunit, *J. Biol. Chem. 268*, 19451−19457.
18. Davare, M. A., Dong, F., Rubin, C. S., and Hell, J. W. (1999) The A-kinase anchor protein MAP2B and cAMP-dependent protein kinase are associated with class C L-type calcium channels in neurons, *J. Biol. Chem. 274*, 30280−30287.
19. Davare, M. A., Horne, M. C., and Hell, J. W. (2000) Protein phosphatase 2A is associated with class C L-type calcium channels ($Ca_v1.2$) and antagonizes channel phosphorylation by cAMP-dependent protein kinase, *J. Biol. Chem. 275*, 39710−39717.
20. Davare, M. A., and Hell, J. W. (2003) Increased phosphorylation of the neuronal L-type Ca^{2+} channel $Ca_v1.2$ during aging, *Proc. Natl. Acad. Sci. U.S.A. 100*, 16018−16023.
21. Gao, T., Yatani, A., Dell'Acqua, M. L., Sako, H., Green, S. A., Dascal, N., Scott, J. D., and Hosey, M. M. (1997) cAMP-dependent regulation of cardiac L-type Ca^{2+} channels requires membrane targeting of PKA and phosphorylation of channel subunits, *Neuron 19*, 185−196.
22. Hell, J. W., Westenbroek, R. E., Elliott, E. M., and Catterall, W. A. (1994) Differential phosphorylation, localization, and function of distinct α1 subunits of neuronal calcium channels. Two size forms for class B, C, and D α1 subunits with different COOH-termini, *Ann. N.Y. Acad. Sci. 747*, 282−293.
23. Hell, J. W., Westenbroek, R. E., Breeze, L. J., Wang, K. K. W., Chavkin, C., and Catterall, W. A. (1996) *N*-Methyl-D-aspartate receptor-induced proteolytic conversion of postsynaptic class C L-type calcium channels in hippocampal neurons, *Proc. Natl. Acad. Sci. U.S.A. 93*, 3362−3367.
24. Wei, X., Neely, A., Lacerda, A. E., Olcese, R., Stefani, E., Perez-Reyes, E., and Birnbaumer, L. (1994) Modification of Ca^{2+} channel activity by deletions at the carboxyl terminus of the cardiac α1 subunit, *J. Biol. Chem. 269*, 1635−1640.
25. Rubin, C. S. (1994) A kinase anchor proteins and the intracellular targeting of signals carried by cyclic AMP, *Biochim. Biophys. Acta 1224*, 467−479.
26. Gray, P. C., Scott, J. D., and Catterall, W. A. (1998) Regulation of ion channels by cAMP-dependent protein kinase and A-kinase anchoring proteins, *Curr. Opin. Neurobiol. 8*, 330−334.
27. Edwards, A. S., and Scott, J. D. (2000) A-kinase anchoring proteins: Protein kinase A and beyond, *Curr. Opin. Cell Biol. 12*, 217−221.
28. Rosenmund, C., Carr, D. W., Bergeson, S. E., Nilaver, G., Scott, J. D., and Westbrook, G. L. (1994) Anchoring of protein kinase A is required for modulation of AMPA/kainate receptors on hippocampal neurons, *Nature 368*, 853−856.
29. Johnson, B. D., Scheuer, T., and Catterall, W. A. (1994) Voltage-dependent potentiation of L-type Ca^{2+} channels in skeletal muscle cells requires anchored cAMP-dependent protein kinase, *Proc. Natl. Acad. Sci. U.S.A. 91*, 11492−11496.
30. Hulme, J. T., Lin, T. W., Westenbroek, R. E., Scheuer, T., and Catterall, W. A. (2003) β-Adrenergic regulation requires direct anchoring of PKA to cardiac $Ca_v1.2$ channels via a leucine zipper interaction with A kinase-anchoring protein 15, *Proc. Natl. Acad. Sci. U.S.A. 100*, 13093−13098.
31. Altier, C., Dubel, S. J., Barrere, C., Jarvis, S. E., Stotz, S. C., Spaetgens, R. L., Scott, J. D., Cornet, V., De Waard, M., Zamponi, G. W., Nargeot, J., and Bourinet, E. (2002) Trafficking of L-type calcium channels mediated by the postsynaptic scaffolding protein AKAP79, *J. Biol. Chem. 277*, 33598−33603.
32. Vallee, R. B., DiBartolomeis, M. J., Theurkauf, W. E. (1981) A protein kinase bound to the projection portion of MAP 2 (microtubule-associated protein 2), *J. Cell. Biol. 90*, 568−576.
33. Ono, K., and Fozzard, H. A. (1992) Phosphorylation restores activity of L-type calcium channels after rundown in inside-out patches from rabbit cardiac cells, *J. Physiol. 454*, 673−688.
34. Csortos, C., Zolnierowicz, S., Bako, E., Durbin, S., and DePaoli-Roach, A. A. (1996) High complexity in the expression of the B′ subunit of protein phosphatase $2A_0$, *J. Biol. Chem. 271*, 2578−2588.
35. Leonard, A. S., Davare, M. A., Horne, M. C., Garner, C. C., and Hell, J. W. (1998) SAP97 is associated with the α-amino-3-hydroxy-5-methylisoxazole-4-propionic acid receptor GluR1 subunit, *J. Biol. Chem. 273*, 19518−19524.
36. Valtschanoff, J. G., Buret, A., Davare, M. A., Leonard, A. S., Hell, J. W., and Weinberg, R. J. (2000) SAP97 concentrates at the postsynaptic density in cerebral cortex, *Eur. J. Neurosci. 12*, 3605−3614.
37. Bennin, D. A., Don, A. S., Brake, T., McKenzie, J. L., Rosenbaum, H., Ortiz, L., DePaoli-Roach, A. A., and Horne, M. C. (2002) Cyclin G2 associates with protein phosphatase 2A catalytic and regulatory B′ subunits in active complexes and induces nuclear aberrations and a G1/S phase cell cycle arrest, *J. Biol. Chem. 277*, 27449−27467.
38. Yang, C. S., Vitto, M. J., Busby, S. A., Garcia, B. A., Kesler, C. T., Gioeli, D., Shabanowitz, J., Hunt, D. F., Rundell, K., Brautigan, D. L., and Paschal, B. M. (2005) Simian virus 40 small t antigen mediates conformation-dependent transfer of protein phosphatase 2A onto the androgen receptor, *Mol. Cell. Biol. 25*, 1298−1308.
39. Brush, M. H., Guardiola, A., Connor, J. H., Yao, T. P., and Shenolikar, S. (2004) Deactylase inhibitors disrupt cellular complexes containing protein phosphatases and deacetylases, *J. Biol. Chem. 279*, 7685−7691.
40. Liang, H., Venema, V. J., Wang, X., Ju, H., Venema, R. C., and Marrero, M. B. (1999) Regulation of angiotensin II-induced phosphorylation of STAT3 in vascular smooth muscle cells, *J. Biol. Chem. 274*, 19846−19851.
41. Jicha, G. A., Weaver, C., Lane, E., Vianna, C., Kress, Y., Rockwood, J., and Davies, P. (1999) cAMP-dependent protein kinase phosphorylations on tau in Alzheimer's disease, *J. Neurosci. 19*, 7486−7494.
42. Strack, S., Cribbs, J. T., and Gomez, L. (2004) Critical role for protein phosphatase 2A heterotrimers in mammalian cell survival, *J. Biol. Chem. 279*, 47732−47739.
43. Dagda, R. K., Zaucha, J. A., Wadzinski, B. E., and Strack, S. (2003) A developmentally regulated, neuron-specific splice variant of the variable subunit Bβ targets protein phosphatase 2A to mitochondria and modulates apoptosis, *J. Biol. Chem. 278*, 24976−24985.
44. Bahl, R., Bradley, K. C., Thompson, K. J., Swain, R. A., Rossie, S., and Meisel, R. L. (2001) Localization of protein Ser/Thr phosphatase 5 in rat brain, *Brain Res. Mol. Brain Res. 90*, 101−109.
45. Snutch, T. P., Tomlinson, W. J., Leonard, J. P., and Gilbert, M. M. (1991) Distinct calcium channels are generated by alternative splicing and are differentially expressed in the mammalian CNS, *Neuron 7*, 45−57.
46. Gao, T., Cuadra, A. E., Ma, H., Bunemann, M., Gerhardstein, B. L., Cheng, T., Eick, R. T., and Hosey, M. M. (2001) C-Terminal fragments of the α 1C ($Ca_v1.2$) subunit associate with and regulate L-type calcium channels containing C-terminal-truncated α 1C subunits, *J. Biol. Chem. 276*, 21089−21097.
47. Leonard, A. S., Lim, I. A., Hemsworth, D. E., Horne, M. C., and Hell, J. W. (1999) Calcium/calmodulin-dependent protein kinase II is associated with the *N*-methyl-D-aspartate receptor, *Proc. Natl. Acad. Sci. U.S.A. 96*, 3239−3244.
48. Yasuda, T., Chen, L., Barr, W., McRory, J. E., Lewis, R. J., Adams, D. J., and Zamponi, G. W. (2004) Auxiliary subunit regulation of high-voltage activated calcium channels expressed in mammalian cells, *Eur. J. Neurosci. 20*, 1−13.
49. Kingston, R. E. (1997) in *Current Protocols in Molecular Biology* (Ausubel, F. M., Brent, R., Kingston, R. E., More, D. D., Seidenman, J. G., Smith, J. A., and Struhl, K., Eds.) pp 9.1.4−9.1.6, John Wiley and Sons, New York.

50. Honkanen, R. E., and Golden, T. (2002) Regulators of serine/threonine protein phosphatases at the dawn of a clinical era? *Curr. Med. Chem. 9*, 2055−2075.
51. Herzig, S., and Neumann, J. (2000) Effects of serine/threonine protein phosphatases on ion channels in excitable membranes, *Physiol. Rev. 80*, 173−210.
52. Huang, H. B., Horiuchi, A., Watanabe, T., Shih, S. R., Tsay, H. J., Li, H. C., Greengard, P., and Nairn, A. C. (1999) Characterization of the inhibition of protein phosphatase-1 by DARPP-32 and inhibitor-2, *J. Biol. Chem. 274*, 7870−7878.
53. Walsh, A. H., Cheng, A., and Honkanen, R. E. (1997) Fostriecin, an antitumor antibiotic with inhibitory activity against serine/threonine protein phosphatases types 1 (PP1) and 2A (PP2A), is highly selective for PP2A, *FEBS Lett. 416*, 230−234.
54. Groblewski, G. E., Wagner, A. C., and Williams, J. A. (1994) Cyclosporin A inhibits Ca^{2+}/calmodulin-dependent protein phosphatase and secretion in pancreatic acinar cells, *J. Biol. Chem. 269*, 15111−15117.
55. Akyol, Z., Bartos, J. A., Merrill, M. A., Faga, L. A., Jaren, O. R., Shea, M. A., and Hell, J. W. (2004) Apo-calmodulin binds with its C-terminal domain to the *N*-methyl-D-aspartate receptor NR1 C0 region, *J. Biol. Chem. 279*, 2166−2175.
56. Klee, C. B., Crouch, T. H., and Krinks, M. H. (1979) Calcineurin: A calcium- and calmodulin-binding protein of the nervous system, *Proc. Natl. Acad. Sci. U.S.A. 76*, 6270−6273.
57. Klee, C. B., Ren, H., and Wang, X. (1998) Regulation of the calmodulin-stimulated protein phosphatase, calcineurin, *J. Biol. Chem. 273*, 13367−13370.
58. Price, N. E., and Mumby, M. C. (1999) Brain protein serine/threonine phosphatases, *Curr. Opin. Neurobiol. 9*, 336−342.
59. Shenolikar, S. (1994) Protein serine/threonine phosphatases—New avenues for cell regulation, *Annu. Rev. Cell Biol. 10*, 55−86.
60. Janssens, V., and Goris, J. (2001) Protein phosphatase 2A: A highly regulated family of serine/threonine phosphatases implicated in cell growth and signalling, *Biochem. J. 353*, 417−439.
61. McCright, B., Rivers, A. M., Audlin, S., and Virshup, D. M. (1996) The B56 family of protein phosphatase 2A (PP2A) regulatory subunits encodes differentiation-induced phosphoproteins that target PP2A to both nucleus and cytoplasm, *J. Biol. Chem. 271*, 22081−22089.
62. Hescheler, J., Kameyama, M., Trautwein, W., Mieskes, G., and Soling, H. D. (1987) Regulation of the cardiac calcium channel by protein phosphatases, *Eur. J. Biochem. 165*, 261−266.
63. Frace, A. M., and Hartzell, H. C. (1993) Opposite effects of phosphatase inhibitors on L-type calcium and delayed rectifier currents in frog cardiac myocytes, *J. Physiol. 472*, 305−326.
64. Hartzell, H. C., Hirayama, Y., and Petit-Jacques, J. (1995) Effects of protein phosphatase and kinase inhibitors on the cardiac L-type Ca current suggest two sites are phosphorylated by protein kinase A and another protein kinase, *J. Gen. Physiol. 106*, 393−414.
65. Wong, W., and Scott, J. D. (2004) AKAP signalling complexes: Focal points in space and time, *Nat. Rev. Mol. Cell Biol. 5*, 959−970.
66. Yan, Z., Hsieh-Wilson, L., Feng, J., Tomizawa, K., Allen, P. B., Fienberg, A. A., Nairn, A. C., and Greengard, P. (1999) Protein phosphatase 1 modulation of neostriatal AMPA channels: Regulation by DARPP-32 and spinophilin, *Nat. Neurosci. 2*, 13−17.
67. Westphal, R. S., Tavalin, S. J., Lin, J. W., Alto, N. M., Fraser, I. D. C., Langeberg, L. K., Sheng, M., and Scott, J. D. (1999) Regulation of NMDA receptors by an associated phosphatase−kinase signaling complex, *Science 285*, 93−96.
68. Pitcher, J. A., Payne, E. S., Csortos, C., DePaoli-Roach, A. A., and Lefkowitz, R. J. (1995) The G-protein-coupled receptor phosphatase: A protein phosphatase type 2A with distinct subcellular distribution and substrate specificity, *Proc. Natl. Acad. Sci. U.S.A. 92*, 8343−8347.
69. Westphal, R. S., Anderson, K. A., Means, A. R., and Wadzinski, B. E. (1998) A signal complex of Ca^{2+}-calmodulin-dependent protein kinase IV and protein phosphatase 2A, *Science 280*, 1258−1261.
70. Marx, S. O., Reiken, S., Hisamatsu, Y., Gaburjakova, M., Gaburjakova, J., Yang, Y. M., Rosemblit, N., and Marks, A. R. (2001) Phosphorylation-dependent regulation of ryanodine receptors: A novel role for leucine/isoleucine zippers, *J. Cell. Biol. 153*, 699−708.
71. Zolnierowicz, S., Van Hoof, C., Andjelkovic, N., Cron, P., Stevens, I., Merlevede, W., Goris, J., and Hemmings, B. A. (1996) The variable subunit associated with protein phosphatase $2A_0$ defines a novel multimember family of regulatory subunits, *Biochem. J. 317* (part 1), 187−194.
72. Strack, S., Ruediger, R., Walter, G., Dagda, R. K., Barwacz, C. A., and Cribbs, J. T. (2002) Protein phosphatase 2A holoenzyme assembly: Identification of contacts between B-family regulatory and scaffolding A subunits, *J. Biol. Chem. 277*, 20750−20755.
73. Terrak, M., Kerff, F., Langsetmo, K., Tao, T., and Dominguez, R. (2004) Structural basis of protein phosphatase 1 regulation, *Nature 429*, 780−784.
74. Gallego, M., and Virshup, D. M. (2005) Protein serine/threonine phosphatases: Life, death, and sleeping, *Curr. Opin. Cell Biol. 17*, 197−202.
75. Coghlan, V. M., Perrino, B. A., Howard, M., Langeberg, L. K., Hicks, J. B., Gallatin, W. M., and Scott, J. D. (1995) Association of protein kinase A and protein phosphatase 2B with a common anchoring protein, *Science 267*, 108−111.
76. Oliveria, S. F., Gomez, L. L., and Dell'Acqua, M. L. (2003) Imaging kinase−AKAP79−phosphatase scaffold complexes at the plasma membrane in living cells using FRET microscopy, *J. Cell. Biol. 160*, 101−112.
77. Herzig, S., Meier, A., Pfeiffer, M., and Neumann, J. (1995) Stimulation of protein phosphatases as a mechanism of the muscarinic-receptor-mediated inhibition of cardiac L-type Ca^{2+} channels, *Pflugers Arch. 429*, 531−538.
78. Victor, R. G., Rusnak, F., Sikkink, R., Marban, E., and O'Rourke, B. (1997) Mechanism of Ca^{2+}-dependent inactivation of L-type Ca^{2+} channels in GH3 cells: Direct evidence against dephosphorylation by calcineurin, *J. Membr. Biol. 156*, 53−61.
79. Schuhmann, K., Romanin, C., Baumgartner, W., and Groschner, K. (1997) Intracellular Ca^{2+} inhibits smooth muscle L-type Ca^{2+} channels by activation of protein phosphatase type 2B and by direct interaction with the channel, *J. Gen. Physiol. 110*, 503−513.
80. Hess, P., Lansman, J. B., and Tsien, R. W. (1984) Different modes of Ca channel gating behaviour favoured by dihydropyridine Ca agonists and antagonists, *Nature 311*, 538−544.
81. Trautwein, W., and Hescheler, J. (1990) Regulation of cardiac L-type calcium current by phosphorylation and G proteins, *Annu. Rev. Physiol. 52*, 257−274.
82. Ono, K., and Fozzard, H. A. (1993) Two phosphatase sites on the Ca^{2+} channel affecting different kinetic functions, *J. Physiol. 470*, 73−84.
83. Wiechen, K., Yue, D. T., and Herzig, S. (1995) Two distinct functional effects of protein phosphatase inhibitors on guinea-pig cardiac L-type Ca^{2+} channels, *J. Physiol. 484*, 583−592.
84. Groschner, K., Schuhmann, K., Mieskes, G., Baumgartner, W., and Romanin, C. (1996) A type 2A phosphatase-sensitive phosphorylation site controls modal gating of L-type Ca^{2+} channels in human vascular smooth-muscle cells, *Biochem. J. 318*, 513−517.

BI051593Z